Acta Math. Univ. Comenianae
Vol. LXVII, 1(1998), pp. 159–179

ADAPTIVE MIXED HYBRID AND MACRO–HYBRID FINITE ELEMENT METHODS

R. H. W. HOPPE AND B. I. WOHLMUTH

Abstract. In this paper, we consider efficient multilevel based iterative solvers and efficient and reliable a posteriori error estimators for mixed hybrid and macro-hybrid finite element discretizations of elliptic boundary value problems. We give an overview concerning the state-of-the-art techniques for these nonconforming approaches and illustrate the performance of the adaptivity concepts realized by some selected numerical examples.

1. Introduction

We consider adaptive mixed hybrid and primal macro-hybrid finite element methods for elliptic boundary value problems. Both approaches have in common that they represent nonconforming discretizations but differ in so far as the first one is based on a dual formulation of the problems under consideration whereas the second one is founded on a macro-hybrid primal variational formulation with respect to a geometrical conforming nonoverlapping decomposition of the computational domain. We note that these techniques have attracted a lot of attention during the last couple of years (cf.,e.g., [**1**], [**2**], [**3**], [**4**], [**7**], [**8**], [**14**], [**15**], [**23**], [**24**]) and are still subject of active research.

In this paper, we will present efficient multilevel preconditioned iterative solvers as well as a posteriori error estimators that may serve as a tool for local adaptive refinement of the triangulations. Both approaches will be outlined for a model problem in terms of a boundary value problem for a linear second order elliptic differential operator in a bounded polygonal or polyhedral domain $\Omega \subset \mathbf{R}^d$, $d = 2$ or $d = 3$

$$Lu := -\nabla \cdot (a\nabla u) + bu = f \quad \text{in } \Omega, \tag{1.1}$$

$$u = 0 \quad \text{on } \Gamma = \partial\Omega, \tag{1.2}$$

Received November 17, 1997.
1980 *Mathematics Subject Classification* (1991 *Revision*). Primary 65N15, 65N30, 65N50, 65N55.
Key words and phrases. Mixed hybrid finite element methods, domain decomposition on nonmatching grids, mortar finite elements, a posteriori error estimators, local adaptive grid refinement.
This work was supported in part by the Deutsche Forschungsgemeinschaft.

where only for simplicity we have chosen homogeneous Dirichlet boundary conditions. The coefficients a and b are assumed to be a symmetric, matrix-valued function $a = (a_{ij})_{i,j=1}^d$, $a_{ij} \in L^\infty(\Omega)$, $1 \leq i, j \leq d$, and a scalar function $b \in L^\infty(\Omega)$ satisfying

$$\underline{\alpha} \mid \xi \mid^2 \leq \sum_{i,j=1}^{d} a_{ij}(x)\xi_i\xi_j \leq \overline{\alpha} \mid \xi \mid^2, \xi \in \mathbf{R}^d, \quad 0 < \underline{\alpha} \leq \overline{\alpha}, \tag{1.3}$$

$$0 \leq \underline{\beta} \leq b(x) \leq \overline{\beta} \tag{1.4}$$

for almost all $x \in \Omega$.

The paper is organized as follows:
In Section 2, we will briefly introduce the idea of mixed hybridization in case of quadrilateral or hexalateral triangulations (cf. subsection 2.1) followed by the construction of a multilevel preconditioned cg-iteration (subsection 2.2). The multilevel solver is based on the equivalence of the mixed hybrid approach with a nonstandard nonconforming primal method in terms of the so-called rotated bilinear resp. trilinear functions. This enables us to utilize multilevel preconditioners designed for the nonconforming setting. Finally, in subsection 2.3 we will introduce an efficient and reliable a posteriori error estimator for the discretization errors both in the primal and dual variables that can be motivated by a superconvergence result known to hold true in the mixed hybrid case.
Section 3 is devoted to adaptive domain decomposition methods on nonmatching grids which are based on the mortar finite element approach that will be described in subsection 3.1. Then, in subsection 3.2 we will sketch the construction of substructuring multilevel preconditioners, whereas in subsection 3.3 we concentrate on the development of a hierarchical type a posteriori error estimator that does provide a lower and an upper bound for the discretization error.
Finally, in Section 4 we will demonstrate the benefits of the adaptive finite element approaches by giving numerical results for some selected illustrative problems.

2. Adaptive Mixed Hybrid Finite Element Methods

2.1 The Mixed Hybrid Approach

Mixed finite element methods are based on a dual formulation of the elliptic boundary value problem (1.1),(1.2). Introducing the flux $\mathbf{j} := a\nabla u$ and the flux space $H(\mathrm{div};\Omega) := \{\mathbf{q} \in L^2(\Omega)^d \mid \mathrm{div}\,\mathbf{q} \in L^2(\Omega)\}$, the elliptic differential equation (1.1) can be formally written as a first order system whose variational formulation gives rise to the following system of variational equations:

Find $(\mathbf{j}, u) \in H(\mathrm{div};\Omega) \times L^2(\Omega)$ such that

$$a(\mathbf{j}, \mathbf{q}) + b(\mathbf{q}, u) = 0, \quad \mathbf{q} \in H(\mathrm{div};\Omega), \tag{2.1}$$

$$b(\mathbf{j}, v) - c(u, v) = -(f, v)_{0;\Omega}, \quad v \in L^2(\Omega), \tag{2.2}$$

where the bilinear forms $a\colon H(\mathrm{div};\Omega)\times H(\mathrm{div};\Omega)\to \mathbf{R}$, $b\colon H(\mathrm{div};\Omega)\times L^2(\Omega)\to \mathbf{R}$ and $c\colon L^2(\Omega)\times L^2(\Omega)\to \mathbf{R}$ are given by

$$\begin{aligned} a(\mathbf{q}_1,\mathbf{q}_2) &:= \int_\Omega a^{-1}\mathbf{q}_1\cdot\mathbf{q}_2\,dx, \mathbf{q}_\nu\in H(\mathrm{div};\Omega),\quad 1\le\nu\le 2,\\ b(\mathbf{q},v) &:= \int_\Omega \mathrm{div}\mathbf{q}v\,dx, \mathbf{q}\in H(\mathrm{div};\Omega),\quad v\in L^2(\Omega),\\ c(v_1,v_2) &:= \int_\Omega bv_1v_2\,dx, v_\nu\in L^2(\Omega),\quad 1\le\nu\le 2. \end{aligned}$$

As usual, we denote by $(\cdot,\cdot)_{k;\Omega}$, $k\ge 0$, the standard inner product on $H^k(\Omega)^d$ and $|\cdot|_{k;\Omega}$, $\|\cdot\|_{k;\Omega}$ stand for the associated seminorms and norms, respectively. We further observe that $H(\mathrm{div};\Omega)$ is a Hilbert space with respect to the graph norm $\|\mathbf{q}\|_{div;\Omega} := (\|\mathbf{q}\|^2_{0;\Omega} + \|\mathrm{div}\mathbf{q}\|^2_{0;\Omega})^{1/2}$.

For the applications in subsection 2.4, we consider a quadrilateral or hexalateral triangulation $\mathcal{T}_h$ of Ω. For $D\subseteq\Omega$, we denote by $\mathcal{N}_h(D),\mathcal{E}_h(D),\mathcal{F}_h(D)$, and $\mathcal{M}_h(D)$ the sets of vertices, edges, faces, and midpoints of edges resp. faces of the triangulation $\mathcal{T}_h$ in D. If $D=\Omega$, we simply write $\mathcal{N}_h$, $\mathcal{E}_h$, $\mathcal{F}_h$, and $\mathcal{M}_h$ and we further refer to $\mathcal{N}_h^{int}$, $\mathcal{E}_h^{int}$, $\mathcal{F}_h^{int}$, and $\mathcal{M}_h^{int}$ as the sets of vertices, edges, faces, and midpoints of edges resp. faces being situated in the interior of Ω. To obtain a unified notation for $d=2$ and $d=3$, we identify the sets of edges and faces in case that $d=2$, i.e. $\mathcal{E}_h$ with $\mathcal{F}_h$ and $\mathcal{E}_h^{int}$ with $\mathcal{F}_h^{int}$. Moreover, $P_k(D)$, $k\ge 0$, stands for the set of polynomials of degree $\le k$ on D.

We approximate the primal variable u by elementwise constants, i.e., we consider the ansatz space

$$W_{[0]}(\Omega;\mathcal{T}_h) := \big\{v_h\in L^2(\Omega)\mid v_h\,|_T\in P_0(T), T\in\mathcal{T}_h\big\}.$$

The corresponding approximation of the flux $\mathbf{j}$ is then given in terms of the lowest order Raviart-Thomas-Nédélec elements $RT_{[0]}(T)$, $T\in\mathcal{T}_h$, given by

$$RT_{[0]}(T) := Q_{1,0,\dots,0}(T)\times\cdots\times Q_{0,\dots,0,1}(T),$$

where $Q_{\alpha_1,\dots,\alpha_d}(T) := \{p\colon T\to\mathbf{R}\mid p(\mathbf{x}) = \sum_{\beta_i\le\alpha_i} a_{\beta_1,\dots,\beta_d}x_1^{\beta_1}\dots x_d^{\beta_d}\}$.

Note that any vector field $\mathbf{q}\in RT_{[0]}(T)$ is uniquely determined by the following degrees of freedom

$$l_F(\mathbf{q}) := \int_F \mathbf{n}\cdot\mathbf{q}\,d\sigma,\quad F\in\mathcal{F}_h(T)$$

so that the dimension of $RT_{[0]}(T)$ is $\dim RT_{[0]}(T) = 2d$ (cf., e.g., [**14**]).

Then, if we choose the global ansatz space according to

$$RT_{[0]}^{-1}(\Omega;\mathcal{T}_h) := \prod_{T\in\mathcal{T}_h} RT_{[0]}(T),$$

we are in a nonconforming situation, since $RT_{[0]}^{-1}(\Omega;\mathcal{T}_h)$ is not a subspace of $H(\mathrm{div};\Omega)$. Indeed, any vector field $\mathbf{q}_h \in RT_{[0]}^{-1}(\Omega;\mathcal{T}_h)$ is in $H(\mathrm{div};\Omega)$ if and only if for all $\mu_h \in L^2(\mathcal{F}_h^{int})$, $\mu_h\,|_F \in P_0(F)$, $F \in \mathcal{F}_h^{int}$

$$\sum_{F\in\mathcal{F}_h^{int}} \int_F \mu_h [\mathbf{n}\cdot\mathbf{q}_h]_J \, d\sigma = 0,$$

where $[\mathbf{n}\cdot\mathbf{q}_h]_J$ denotes the jump of the normal component of $\mathbf{q}_h$ across the interelement boundaries.

Therefore, in order to establish consistency of the nonconforming approach we impose continuity constraints on the interelement boundaries by means of Lagrangian multipliers from the multiplier space

$$M_{[0]}(\Omega;\mathcal{F}_h^{int}) := \left\{\mu_h \in L^2(\mathcal{F}_h^{int}) \mid \mu_h\,|_F \in P_0(F), \quad F \in \mathcal{F}_h^{int}\right\}.$$

Introducing the bilinear form $d\colon M_{[0]}(\Omega;\mathcal{F}_h^{int}) \times RT_{[0]}^{-1}(\Omega;\mathcal{T}_h) \to \mathbf{R}$ according to

$$d(\mu_h,\mathbf{q}_h) := -\sum_{F\in\mathcal{F}_h^{int}} \int_F \mu_h [\mathbf{n}\cdot\mathbf{q}_h]_J \, d\sigma, \quad \mu_h \in M_{[0]}(\Omega;\mathcal{F}_h^{int}), \quad \mathbf{q}_h \in RT_{[0]}^{-1}(\Omega;\mathcal{T}_h),$$

the mixed hybrid finite element approximation of (1.1), (1.2) is:
Find $(\mathbf{j_h}, u_h, \lambda_h) \in RT_{[0]}^{-1}(\Omega;\mathcal{T}_h) \times W_{[0]}(\Omega;\mathcal{T}_h) \times M_{[0]}(\Omega;\mathcal{F}_h^{int})$ such that

$$a(\mathbf{j_h},\mathbf{q}_h) + b(\mathbf{q}_h,u_h) + d(\lambda_h,\mathbf{q}_h) = 0, \quad \mathbf{q}_h \in RT_{[0]}^{-1}(\Omega;\mathcal{T}_h), \tag{2.3}$$

$$b(\mathbf{j_h},v_h) - c(u_h,v_h) = -(f,v_h)_{0;\Omega}, \quad v_h \in W_{[0]}(\Omega;\mathcal{T}_h), \tag{2.4}$$

$$d(\mu_h,\mathbf{j_h}) = 0, \mu_h \in M_{[0]}(\Omega;\mathcal{F}_h^{int}). \tag{2.5}$$

Note that the idea of mixed hybridization is due to Fraeijs de Veubeke [**18**]. Analytical investigations including a priori error estimates and postprocessing techniques have been done by Arnold and Brezzi [**5**] (cf. also [**14**]).

2.2 Multilevel Iterative Solvers

Identifying vector-valued and scalar finite element functions with vector fields and vectors, respectively, in its algebraic form the saddle point problem (2.3), (2.4), (2.5) gives rise to the linear system

$$\begin{pmatrix} A_h & B_h^T & D_h^T \\ B_h & -C_h & 0 \\ D_h & 0 & 0 \end{pmatrix} \begin{pmatrix} \mathbf{j_h} \\ u_h \\ \lambda_h \end{pmatrix} = \begin{pmatrix} 0 \\ -f_h \\ 0 \end{pmatrix} \tag{2.6}$$

with a symmetric, but indefinite 3×3 block coefficient matrix. Since A_h represents a blockdiagonal matrix with $2d \times 2d$ blocks in the diagonal and $E_h := C_h +$

$B_h A_h^{-1} B_h^T$ turns out to be a diagonal matrix, static condensation of both the discrete flux $\mathbf{j_h}$ and the discrete primal variable u_h in (2.6) can be easily performed. Setting $G_h := D_h A_h^{-1} B_h^T$, this yields the linear system

$$S_h \lambda_h = -G_h E_h^{-1} f_h \tag{2.7}$$

with the symmetric, positive definite Schur complement $S_h := D_h A_h^{-1} D_h^T - G_h E_h^{-1} G_h^T$ (see [**14**]). The efficient iterative solution of the saddle point problem (2.6) resp. the Schur complement system (2.7) will be based on the fact that it is equivalent to a modified nonstandard nonconforming primal approach obtained by the so-called rotated bilinears ($d = 2$) resp. trilinears ($d = 3$) (cf., e.g., [**19**], [**27**]).

In particular, the rotated elements resulting from a rotation in the (x_i, x_{i+1})-plane by 45^0 are given by

$$\tilde{Q}_1(T) := \{1, x_i, x_{i+1}, x_i^2 - x_{i+1}^2 \mid 1 \le i \le d-1\}.$$

Note that any function $v \in \tilde{Q}_1(T)$ is uniquely determined by the following degrees of freedom

$$l_F(v) := \frac{1}{|F|} \int\limits_F v \, d\sigma, \quad F \in \mathcal{F}_h(T),$$

where $|F|$ denotes the area of F.

Then the global nonconforming ansatz space is as follows

$$\begin{aligned} RML_{[1]}(\Omega; \mathcal{T}_h) := \Big\{ & v_h \in L^2(\Omega) \mid v_h \mid_T \in \tilde{Q}_1(T), T \in \mathcal{T}_h, \\ & l_F(v|_T) = l_F(v|_{T'}) \text{ if } F = \partial T \cap \partial T' \text{ and} \\ & l_F(v|_T) = 0 \text{ if } F \subset \partial T \cap \partial \Omega \Big\}. \end{aligned}$$

The modification consists in an enrichment of $RML_{[1]}(\Omega; \mathcal{T}_h)$ according to

$$NC_{[1]}(\Omega; \mathcal{T}_h) := RML_{[1]}(\Omega; \mathcal{T}_h) \oplus B_2(\Omega; \mathcal{T}_h), \tag{2.8}$$

where $B_2(\Omega; \mathcal{T}_h)$ stands for the space of elementwise d-quadratic bubble functions vanishing on the boundary of the elements

$$B_2(\Omega; \mathcal{T}_h) := \{v_h \in L^2(\Omega) \mid v_h \mid_T \in Q_{2,\ldots,2}(T), v_h \mid_{\partial T} = 0\}.$$

We further denote by P the orthogonal L^2-projection $P\colon L^2(\Omega) \to W_{[0]}(\Omega; \mathcal{T}_h)$, by $P_{a^{-1}}$ the weighted L^2-projection $P_{a^{-1}} : L^2(\Omega)^d \to RT_{[0]}^{-1}(\Omega; \mathcal{T}_h)$ given by

$$\int_\Omega a^{-1} (P_{a^{-1}} \mathbf{q}) \cdot \mathbf{p} \, dx = \int_\Omega a^{-1} \mathbf{q} \cdot \mathbf{p} \, dx, \mathbf{q} \in L^2(\Omega)^d, \mathbf{p} \in RT_{[0]}^{-1}(\Omega; \mathcal{T}_h),$$

and by $\hat{P}$ the orthogonal projection $\hat{P}\colon NC_{[1]}(\Omega;\mathcal{T}_h) \to M_{[0]}(\Omega;\mathcal{F}_h^{int})$ according to

$$\int_F (\hat{P}u_h)v_h \, d\sigma = \int_F u_h v_h \, d\sigma, \quad F \in \mathcal{F}_h^{int}, \quad v_h \in P_0(F).$$

We recall that $\int_F u_h v_h d\sigma$, $v_h \in P_0(F)$ is well defined because of the definition of the global ansatz space $NC_{[1]}(\Omega;\mathcal{T}_h)$. We introduce the bilinear form $a_{NC}\colon NC_{[1]}(\Omega;\mathcal{T}_h) \times NC_{[1]}(\Omega;\mathcal{T}_h) \to \mathbf{R}$ by

$$a_{NC}(u_h, v_h) := \sum_{T\in\mathcal{T}_h} \int_T (P_{a^{-1}}(a\nabla u_h)\cdot \nabla v_h + b(Pu_h)(Pv_h))\, dx,$$

and we consider the following nonconforming primal finite element approximation of (1.1), (1.2): Find $u_{NC} \in NC_{[1]}(\Omega;\mathcal{T}_h)$ such that

$$a_{NC}(u_{NC}, v_h) = (Pf, v_h)_{0;\Omega}, v_h \in NC_{[1]}(\Omega;\mathcal{T}_h). \tag{2.9}$$

There is a close relationship between the mixed hybrid approach (2.3), (2.4), (2.5) and (2.9):

Theorem 2.1. *Let* $(\mathbf{j_h}, u_h, \lambda_h) \in RT_{[0]}^{-1}(\Omega;\mathcal{T}_h) \times W_{[0]}(\Omega;\mathcal{T}_h) \times M_{[0]}(\Omega;\mathcal{F}_h^{int})$ *and* $u_{NC} \in NC_{[1]}(\Omega;\mathcal{T}_h)$ *be the unique solutions of* (2.3), (2.4), (2.5) and (2.9), *respectively. Then there holds*

$$P_{a^{-1}}(a\nabla u_{NC}) = \mathbf{j_h}, \quad Pu_{NC} = u_h, \quad \hat{P}u_{NC} = \lambda_h. \tag{2.10}$$

Proof. The assertion follows easily by verifying that $\mathbf{j_h}, u_h$, and λ_h as given by (2.10) satisfy the variational equations (2.3), (2.4) and (2.5). □

We can take advantage of the equivalence stated in the previous theorem by using an efficient multilevel preconditioner for the preconditioned cg-iterative solution of the nonconforming primal approximation (2.9). In particular, due to the fact that the stiffness matrix associated with the bilinear form $a_{NC}(\cdot,\cdot)$ is spectrally equivalent to its blockdiagonal and using basic properties of the projection operators $P_{a^{-1}}$ and P, an appropriate preconditioner is given by

$$\mathcal{R}_{NC} = \begin{pmatrix} R_{RML} & 0 \\ 0 & R_{B_2} \end{pmatrix}. \tag{2.11}$$

Here R_{RML} is a preconditioner for the stiffness matrix A_{RML} associated with the bilinear form

$$a_{RML}(u_h, v_h) := \sum_{T\in\mathcal{T}_h} \int_T (a\nabla u_h \cdot \nabla v_h + b u_h v_h)\, dx, \quad u_h, v_h \in RML_{[1]}(\Omega;\mathcal{T}_h),$$

and R_{B_2} is a preconditioner for the stiffness matrix A_{B_2} induced by the bilinear form

$$a_{B_2}(u_h,v_h) := \sum_{T\in\mathcal{T}_h}\int_T (aP_{Id}(\nabla u_h)\cdot P_{Id}(\nabla v_h)+bPu_hPv_h)\,dx,\quad u_h,v_h\in B_2(\Omega;\mathcal{T}_h).$$

A detailed proof of the spectral equivalence in case of simplicial triangulations is given in [**22**]. Since the bubble functions spanning $B_2(\Omega;\mathcal{T}_h)$ are strictly local, A_{B_2} is a diagonal matrix and we may thus take $R_{B_2}=A_{B_2}$. Therefore, it only remains to specify an appropriate preconditioner R_{RML} for A_{RML}. For that purpose, we assume that we are given a hierarchy $(\mathcal{T}_k)_{k=0}^{j}$ of quadrilateral or hexalateral triangulations generated by the adaptive refinement process that will be described in the following subsection. We denote by $(RML_{[1]}(\Omega;\mathcal{T}_k))_{k=0}^{j}$ the associated sequence of finite element spaces in terms of the rotated bi- resp. trilinears with respect to the triangulations $\mathcal{T}_k$, $0\le k\le j$. As with all nonconforming approximations we are then faced with the problem that this sequence is nonnested. We note that in case of simplicial triangulations appropriate remedies have been suggested in [**13**], [**26**], and by the authors [**22**]. Here, we will follow the approach in [**22**] and adopt a pseudo-interpolation operator originally due to Sarkis [**28**]. The nonconforming finite element space $RML_{[1]}(\Omega;\mathcal{T}_j)$ can be identified with a closed subspace of a conforming counterpart. This enables us to construct a multilevel preconditioner by means of the BPX-preconditioner (cf., e.g., [**11**], [**33**]) for the associated sequence of conforming finite element spaces.

We denote by $\widetilde{\mathcal{T}}_{j+1}$ the triangulation obtained from $\mathcal{T}_j$ by uniform refinement and we refer to $S_1(\Omega;\widetilde{\mathcal{T}}_{j+1})$ as the finite element space associated with the standard conforming P1 approximation of (1.1), (1.2) with respect to $\widetilde{\mathcal{T}}_{j+1}$. We define the pseudo-interpolation operator $P_{RML}\colon RML_{[1]}(\Omega;\mathcal{T}_j)\to S_1(\Omega;\widetilde{\mathcal{T}}_{j+1})$ according to

$$(P_{RML}v_j)(p) := \begin{cases} l_F(v_j) & \text{if } p=m_F\in\mathcal{M}_j^{int}\subset\widetilde{\mathcal{N}}_{j+1}^{int}\\ \frac{1}{\nu_p}\sum\limits_{\nu=1}^{\nu_p} l_{F_\nu^p}(v_j) & \text{if } p\in\widetilde{\mathcal{N}}_{j+1}^{int}\setminus\mathcal{M}_j^{int}\end{cases},$$

where ν_p is the number of edges $(d=2)$ and faces $(d=3)$ emanating from $p\in\widetilde{\mathcal{N}}_{j+1}^{int}\setminus\mathcal{M}_j^{int}$ and $F_\nu^p\in\mathcal{M}_j$, $1\le\nu\le\nu_p$, stand for the corresponding edges and faces.

We denote by R_{BPX} the BPX-preconditioner with respect to the nested hierarchy $S_1(\Omega;\mathcal{T}_0)\subset\cdots\subset S_1(\Omega;\widetilde{\mathcal{T}}_{j+1})$ and by $P_{RML}^{+}\colon S_1(\Omega;\widetilde{\mathcal{T}}_{j+1})\to RML_{[1]}(\Omega;\mathcal{T}_j)$ the pseudo-inverse of the pseudo-interpolation operator P_{RML}. Then the nonconforming BPX-type preconditioner R_{RML} is given by means of

$$R_{RML}^{-1} := P_{RML}^{+}R_{BPX}^{-1}(P_{RML}^{+})^{T}. \tag{2.12}$$

We remark that in its algebraic form the pseudo-inverse P_{RML}^{+} represents an $m_j\times n_{j+1}$ rectangular matrix of the form

$$P_{RML}^{+} = (I\quad 0),$$

where $m_j := \dim RML_{[1]}(\Omega;\mathcal{T}_j)$, $n_{j+1} := \dim S_1(\Omega;\widetilde{\mathcal{T}}_{j+1})$ and I stands for the $m_j \times m_j$ identity matrix. Thus P_{RML}^{+} and $(P_{RML}^{+})^T$ are easily computable and R_{RML}^{-1} is of the same arithmetical complexity as R_{BPX}^{-1}.

Theorem 2.2. *Let R_{RML} be given by means of (2.12). Then there exist constants $0 < \gamma_{RML} \le \Gamma_{RML}$ depending only on the ellipticity constants and on the local geometry of $\mathcal{T}_0$ such that*

$$\gamma_{RML} I \le R_{RML}^{-1} A_{RML} \le \Gamma_{RML} I. \tag{2.13}$$

Proof. The assertion can be proved by using Nepomnyaschikh's fictitious domain lemma [**25**]. The proof follows the same lines as in the case of hierarchies of simplicial triangulations (cf. [**22**]). □

As an immediate consequence of the preceding result we obtain:

Corollary 2.3. *Let $\mathcal{A}_{NC}$ be the stiffness matrix associated with the bilinear form a_{NC} partitioned according to the splitting (2.8) of $NC_{[1]}(\Omega;\mathcal{T}_j)$. Further, let $\mathcal{R}_{NC}$ be given by (2.11) with R_{RML} as in (2.12) and $R_{B_2} = A_{B_2}$. Then there exist constants $0 < \gamma_{NC} \le \Gamma_{NC}$ depending only on the ellipticity constants and on the local geometry of $\mathcal{T}_0$ such that*

$$\gamma_{NC} I \le \mathcal{R}_{NC}^{-1} \mathcal{A}_{NC} \le \Gamma_{NC} I. \tag{2.14}$$

2.3 A Posteriori Error Estimation and Adaptive Refinement

Local adaptive refinement of the triangulations can be performed by means of an a posteriori error estimator for the discretization error $e_u := u - u_h$ in the primal variable measured in the L^2-norm and the discretization error $\mathbf{e}_j := \mathbf{j} - \mathbf{j_h}$ in the fluxes measured in the $H(\mathrm{div}\,;\Omega)$-norm.

The estimator for the error in the primal variable is based on the following superconvergence result:

Lemma 2.1. *Let $u_h \in W_{[0]}(\Omega;\mathcal{T}_h)$ be the elementwise constant approximation of the primal variable $u \in L^2(\Omega)$ and let $\hat{u}_h$ be the nonconforming extension of the interelement multiplier $\lambda_h \in M_{[0]}(\Omega;\mathcal{T}_h)$. Then, under the regularity assumptions $u \in H^2(\Omega)$, $f \in H^1(\Omega)$ there holds*

$$\|u - u_h\|_{0;\Omega} \le Ch, \quad \|u - \hat{u}_h\|_{0;\Omega} \le Ch^2. \tag{2.15}$$

Proof. The proof is similar to that in case of simplicial triangulations (cf., e.g., [**14**]). □

The preceding result (2.15) motivates the saturation assumption

$$\|u - \hat{u}_h\|_{0;\Omega} \leq \beta \|u - u_h\|_{0;\Omega}, \quad 0 \leq \beta < 1 \tag{2.16}$$

which implies that $\|u_h - \hat{u}_h\|_{0;\Omega}$ provides a lower and an upper bound for the discretization error in the primal variable

$$(1+\beta)^{-1}\|u_h - \hat{u}_h\|_{0;\Omega} \leq \|u - u_h\|_{0;\Omega} \leq (1-\beta)^{-1}\|u_h - \hat{u}_h\|_{0;\Omega}.$$

An estimator for the discretization error in the fluxes can be obtained by means of an interpolation operator $\mathbf{K}\colon RT_{[0]}^{-1}(\Omega;\mathcal{T}_h) \to RML_{[1]}(\Omega;\mathcal{T}_h)^d$ due to Brandts [**12**] which is locally defined by

$$\int_F \mathbf{Kq}\, d\sigma := \frac{1}{2}\int_F (\mathbf{q}\,|_{T_1} + \mathbf{q}\,|_{T_2})\, d\sigma, \quad \partial T_1 \cap \partial T_2 = F \in \mathcal{F}_h^{int},$$
$$\int_F \mathbf{t}\cdot\mathbf{Kq}\, d\sigma := 0, \quad \int_F \mathbf{n}\cdot\mathbf{Kq}\, d\sigma := \int_F \mathbf{n}\cdot\mathbf{q}\,|_{T_F}\; d\sigma, \quad F \subset \partial T_F \cap \Gamma,$$

where $\mathbf{t}$ is an abitrary vector orthogonal to $\mathbf{n}$. The error term $\|\mathbf{j_h} - \mathbf{Kj_h}\|_{0;\Omega}$ then provides an estimate of the discretization error in the fluxes. Combining both estimators we obtain

$$\eta_S^2 := \sum_{T\in\mathcal{T}_h} \eta_{S;T}^2, \tag{2.17}$$

$$\eta_{S;T}^2 := \|\mathbf{j_h} - \mathbf{Kj_h}\|_{0;\Omega}^2 + \|u_h - \hat{u}_h\|_{0;T}^2 + \|f - \pi_0 f\|_{0;T}^2, \tag{2.18}$$

where $\pi_0 f$ stands for the L^2-projection of the right-hand side f onto $W_{[0]}(\Omega;\mathcal{T}_h)$.

Theorem 2.4. *Let η_S be given by means of* (2.17), (2.18). *Under appropriate regularity assumptions and* (2.16) *there exist constants $0 < \gamma_S \leq \Gamma_S$ depending only on the ellipticity constants and on the shape regularity of the triangulation such that*

$$\gamma_S \eta_S^2 \leq \|u - u_h\|_{0;\Omega}^2 + \|\mathbf{j} - \mathbf{j_h}\|_{div;\Omega}^2 \leq \Gamma_S \eta_S^2. \tag{2.19}$$

Proof. The proof is virtually the same as in case of simplicial triangulations (cf., e.g., [**12**], [**22**]). □

We remark that in practice we only have approximations $\tilde{u}_h$ for u_h and $\tilde{\mathbf{j}}_\mathbf{h}$ for $\mathbf{j_h}$ at hand and thus want to estimate the total errors $u - \tilde{u}_h$ and $\mathbf{j} - \tilde{\mathbf{j}}_\mathbf{h}$. In this case, the iteration errors $\|u_h - \tilde{u}_h\|_{0;\Omega}$ and $\|\mathbf{j_h} - \tilde{\mathbf{j}}_\mathbf{h}\|_{div;\Omega}$ additionally enter the estimator η_S. However, due to the fact that $\tilde{u}_h$ and $\tilde{\mathbf{j}}_\mathbf{h}$ are determined by means of an optimal multilevel preconditioned cg-iteration, the iteration errors can be controlled within the iterative solution process, for instance, by monitoring the residuals with respect to the iterates.

A final remark is due to the refinement process. We compute the average of the local error terms

$$\eta_{av}^2 := \frac{1}{N_h} \sum_{T \in \mathcal{T}_h} \eta_{S;T}^2,$$

where $N_h := \operatorname{card}\{T \mid T \in \mathcal{T}_h\}$ and mark an element $T \in \mathcal{T}_h$ for refinement if

$$\eta_{S;T}^2 \geq \sigma \eta_{av}^2$$

with $\sigma > 0$ being an appropriate safety factor (e.g. $\sigma \approx 0.9$).

An element $T \in \mathcal{T}_h$ marked for refinement will be subdivided into four $(d = 2)$ resp. eight $(d = 3)$ congruent subelements. We note that nonconforming nodal points arising from that refinement are treated in the standard way as slave nodes within the subsequent iterative solution process.

3. Adaptive Domain Decomposition on Nonmatching Grids

3.1 The Mortar Finite Element Approach

For the elliptic boundary value problem (1.1), (1.2) in a bounded polygonal domain $\Omega \subset \mathbf{R}^2$, we consider a decomposition

$$\overline{\Omega} = \bigcup_{i=1}^{N} \overline{\Omega}_i, \quad \Omega_i \cap \Omega_j = \emptyset, \quad 1 \leq i \neq j \leq N, \tag{3.1}$$

Ω into N mutually disjoint, polygonal subdomains Ω_i. We assume that this partition is geometrically conforming in the sense that any edge of $\partial\Omega_i, 1 \leq i \leq N$ is either part of the boundary $\partial\Omega$ of the entire domain Ω or coincides with an edge of an adjacent subdomain of the partition. We refer to

$$S = \bigcup_{i=1}^{N} (\partial\Omega_i \setminus \partial\Omega) = \bigcup \{\Gamma_{ij} := \partial\Omega_i \cap \partial\Omega_j \mid \Gamma_{ij} \neq \emptyset\} \tag{3.2}$$

as the skeleton of the decomposition and define

$$X(\Omega) := \left\{ v \in \prod_{i=1}^{N} H^1(\Omega_i) \,\Big|\, \sum_{\Gamma_{ij}} \int_{\Gamma_{ij}} \lambda [v]_J \, d\sigma = 0, \ \lambda \in H^{-1/2}(S), \ v \,|_{\Gamma} = 0 \right\}, \tag{3.3}$$

where $[v]_J$ denotes the jump of v across $\Gamma_{ij} \in S$.

Then, the macro-hybrid variational formulation of (1.1), (1.2) with respect to the decomposition (3.1) is:
Find $u \in X(\Omega)$ such that

$$a(u,v) = (f,v)_{0;\Omega}, \quad v \in X(\Omega), \tag{3.4}$$

where

$$a(u,v) := \sum_{i=1}^{N} a_i(u,v), a_i(u,v) := \int_{\Omega_i} (a\nabla u \cdot \nabla v + buv)\, dx, \quad 1 \le i \le N.$$

We further consider individual simplicial triangulations $\mathcal{T}_i$ of the subdomains Ω_i, $1 \le i \le N$, and denote by

$$S_1(\Omega_i;\mathcal{T}_i) := \big\{ v \in H^1(\Omega_i) \mid v\,|_T \in P_1(T), T \in \mathcal{T}_i, v\,|_{\partial\Omega_i \cap \partial\Omega} = 0, \text{ if } \partial\Omega_i \cap \partial\Omega \ne \emptyset \big\}$$

the standard conforming P1 finite element space with respect to $\mathcal{T}_i$.

We decompose the skeleton S according to

$$S = \bigcup_{l=1}^{L} \overline{\gamma}_l, \quad \gamma_l \cap \gamma_m = \emptyset, \quad 1 \le l \ne m \le L \tag{3.5}$$

into the so-called mortars $\gamma_l, 1 \le l \le L$, where each mortar γ_l is the entire open edge of some subdomain $\Omega_{M(l)}$, $M(l) \in \{1, \ldots, N\}$. We denote by $\Omega_{\overline{M(l)}}$ the adjacent subdomain and refer to its corresponding edge as the nonmortar Γ_l. This formal distinction between mortars and nonmortars is essential, since due to the different triangulations of the trace spaces

$$\begin{aligned} W_{M(l)}(\gamma_l) &:= \big\{ v\,|_{\gamma_l} \mid v \in S_1(\Omega_{M(l)}, \mathcal{T}_{M(l)}) \big\}, \\ W_{\overline{M(l)}}(\Gamma_l) &:= \big\{ v\,|_{\Gamma_l} \mid v \in S_1(\Omega_{\overline{M(l)}}, \mathcal{T}_{\overline{M(l)}}) \big\} \end{aligned}$$

do not necessarily coincide. We denote the outer unit normal vector on $\Omega_{\overline{M(l)}}$ by $\mathbf{n}$ whereas $\mathbf{n}_i$ stands for the outer unit normal vector on Ω_i. Then, the jump on Γ_l is defined by $[v]_J := v|_{\Omega_{\overline{M(l)}}} - v|_{\Omega_{M(l)}}$.

We impose weak continuity constraints on the internal subdomain boundaries by means of Lagrangian multipliers from the multiplier space

$$\begin{aligned} M_1(S) := \Big\{ &\mu \in L^2(S) \mid \exists v \in S_1(\Omega_{\overline{M(l)}}, \mathcal{T}_{\overline{M(l)}}),\ 1 \le l \le L, \\ &\mu\,|_{\Gamma_l} = v\,|_{\Gamma_l}, \mu\,|_E \in P_0(E), E \cap \partial\Gamma_l \ne \emptyset \Big\} \end{aligned}$$

where E are the edges of the nonmortar faces Γ_l. Note that $\{\mu\,|_{\Gamma_l} \mid \mu \in M_1(S)\}$ is a subspace of $W_{\overline{M(l)}}(\Gamma_l)$ of codimension 2.

We define

$$X_1(\Omega;\mathcal{T}) := \left\{ v \in \prod_{i=1}^N S_1(\Omega_i;\mathcal{T}_i) \;\Big|\; \sum_{l=1}^L \int_{\Gamma_l} \mu[v]_J \, d\sigma = 0, \quad \mu \in M_1(S) \right\}. \tag{3.6}$$

Then, the mortar finite element approximation of (1.1), (1.2) amounts to the computation of $u_m \in X_1(\Omega;\mathcal{T})$ such that

$$a(u_m, v) = (f, v)_{0;\Omega}, \quad v \in X_1(\Omega;\mathcal{T}). \tag{3.7}$$

We note that (3.8) can be equivalently stated as a saddle point problem. Introducing the bilinear form

$$b(\mu, v) := -\sum_{l=1}^L \int_{\Gamma_l} \mu[v]_J \, d\sigma, \quad \mu \in M_1(S), \quad v \in \prod_{i=1}^N H^1(\Omega_i),$$

we are looking for a pair $(u_m, \lambda_m) \in \prod_{i=1}^N S_1(\Omega_i;\mathcal{T}_i) \times M_1(S)$ satisfying

$$a(u_m, v) + b(\lambda_m, v) = (f, v)_{0;\Omega}, \quad v \in \prod_{i=1}^N S_1(\Omega_i;\mathcal{T}_i), \tag{3.8}$$

$$b(\mu, u_m) = 0, \quad \mu \in M_1(S). \tag{3.9}$$

In particular, (3.8), (3.9) satisfies the Babuška-Brezzi condition and the existence and uniqueness of a solution is guaranteed (cf., e.g., [**8**], [**9**]). Note that the Lagrangian multiplier $\lambda_M \in M_1(S)$ provides an approximation of the normal flux $\mathbf{n} \cdot a\nabla u$ on the skeleton S of the decomposition.

3.2 Multilevel Preconditioned Iterative Solvers

The algebraic form of the saddle point problem (3.8), (3.9) is given by the linear system

$$\mathcal{A} \begin{pmatrix} u_m \\ \lambda_m \end{pmatrix} = \begin{pmatrix} A & B^T \\ B & 0 \end{pmatrix} \begin{pmatrix} u_m \\ \lambda_m \end{pmatrix} = \begin{pmatrix} b \\ 0 \end{pmatrix}, \tag{3.10}$$

where the first diagonal block A of the stiffness matrix $\mathcal{A}$ is a blockdiagonal matrix $A = \operatorname{diag}(A_1, \ldots A_N)$ with A_i, $1 \le i \le N$, referring to the $n_i \times n_i$ subdomain stiffness matrices, $n_i := \dim S_1(\Omega_i;\mathcal{T}_i)$. The offdiagonal blocks B and B^T represent the continuity constraints on the skeleton.

We will solve (3.10) by preconditioned Lanczos iterations with a blockdiagonal preconditioner

$$\mathcal{R} := \begin{pmatrix} R_u & 0 \\ 0 & R_\lambda \end{pmatrix}, \tag{3.11}$$

where $R_u := \operatorname{diag}(R_1, \ldots, R_N)$ consists of preconditioners R_i, $1 \le i \le N$, for the subdomain stiffness matrices A_i and R_λ is a preconditioner for the Schur complement $S_\lambda := BA^{-1}B^T$.

We will construct subdomain preconditioners R_i, $1 \le i \le N$, and a preconditioner R_λ for the Schur complement S_λ with respect to hierarchies $(\mathcal{T}_i^{(k)})_{k=0}^K$ of nonuniform triangulations of the subdomains Ω_i such that the spectral condition numbers of the preconditioned matrices are independent of the refinement level. In particular, a natural candidate for the preconditioners R_i, $1 \le i \le N$, is the BPX-preconditioner (cf.,e.g., [**11**], [**33**]). We may also use a BPX-type preconditioner for the Schur complement. Indeed, taking advantage of the decomposition

$$A_i = \begin{pmatrix} A_{II}^{(i)} & A_{I\Gamma}^{(i)} \\ A_{\Gamma I}^{(i)} & A_{\Gamma\Gamma}^{(i)} \end{pmatrix}, \qquad B_i^T = \begin{pmatrix} 0 \\ (B_{\Gamma\Gamma}^{(i)})^T \end{pmatrix}$$

of the matrices A_i and B_i^T with I and Γ referring to interior and boundary nodal points, respectively, we have a corresponding partition of S_λ according to

$$S_\lambda = \sum_{i=1}^N B_{\Gamma\Gamma}^{(i)} (S_{\Gamma\Gamma}^{(i)})^{-1} (B_{\Gamma\Gamma}^{(i)})^T, \tag{3.12}$$

where $S_{\Gamma\Gamma}^{(i)} := A_{\Gamma\Gamma}^{(i)} - A_{\Gamma I}^{(i)}(A_{II}^{(i)})^{-1}A_{I\Gamma}^{(i)}$, $1 \le i \le N$ are the individual subdomain Schur complements. We obtain a Schur complement preconditioner R_λ, if in (3.12) we replace $(S_{\Gamma\Gamma}^{(i)})^{-1}$ by $(R_{\Gamma\Gamma}^{(i)})^{-1}$ where $R_{\Gamma\Gamma}^{(i)}$ can be constructed by means of the boundary diagonal blocks of the BPX-preconditioners. For a more detailed discussion of this issue we refer to [**17**], [**23**].

3.3 A Hierarchical Type a Posteriori Error Estimator

We construct a hierarchical basis a posteriori error estimator by a localization of the defect equation on the subdomains' level replacing the unknown normal fluxes on the skeleton by the available multiplier $\lambda_M \in M_1(S)$. The resulting Neumann problems are then solved by using the standard conforming P2 approximation on the individual subdomains and performing a further localization by means of the hierarchical two-level splitting of the higher order finite element spaces. We note that this technique can be interpreted as a hybrid approach with respect to the hierarchical type a posteriori error estimation concepts as developed by Bank and Weiser [**6**] and by Deuflhard, Leinen, and Yserentant [**16**]. We further remark that hierarchical type a posteriori error estimators for standard nonconforming finite element discretizations of elliptic boundary value problems have been established by the authors in [**20**], [**21**].

We assume that $(\mathcal{T}_i^{(k)})_{k \in \mathbf{N}_0}$ are regular, locally quasiuniform, nested sequences of simplicial triangulations of Ω_i, $1 \le i \le N$. We denote by $\mathcal{E}_k^{(D)}$ the sets of edges of $\mathcal{T}_k = \cup_{i=1}^N \mathcal{T}_i^{(k)}$ in $D \subseteq \Omega$ and by $0 < c \le C$ generic constants that only depend on the shape regularity of $\mathcal{T}_i^{(0)}$, $1 \le i \le N$, and possibly on the constants $\underline{\alpha}, \overline{\alpha}, \underline{\beta}, \overline{\beta}$ in (1.3), (1.4).

Assuming that the solution u of the macro-hybrid variational formulation (3.4) satisfies $u \in \prod_{i=1}^N H^2(\Omega_i)$ and $[\mathbf{n} \cdot a\nabla u]_J = 0$ on S, it is easy to see that the discretization error $e := u - u_m$ solves the variational equation

$$a(e, v) = r(v), \quad v \in \prod_{i=1}^N H^1(\Omega_i), \tag{3.13}$$

where the residual $r(\cdot)$ is given by

$$r(v) := (f, v)_{0;\Omega} - b(\mathbf{n} \cdot a\nabla u, v) - a(u_m, v). \tag{3.14}$$

Now, setting $e_i := e\,|_{\Omega_i}, 1 \le i \le N$, we obtain from (3.13)

$$a_i(e_i, v) = (f, v)_{0;\Omega_i} - a_i(u_m, v) + \int\limits_{\partial\Omega_i \setminus \partial\Omega} \mathbf{n}_i \cdot a\nabla u v \, d\sigma, \quad v \in H^1(\Omega_i). \tag{3.15}$$

We replace the unknown normal fluxes $\mathbf{n} \cdot a\nabla u$ in (3.15) by the available Lagrangian multiplier λ_m and approximate the resulting Neumann problems by using the finite element spaces $S_2(\Omega_i; \mathcal{T}_i^{(k)})$, $1 \le i \le N$, of continuous, piecewise quadratic finite elements:

Find $\tilde{e}_i \in S_2(\Omega_i; \mathcal{T}_i^{(k)})$ such that

$$a_i(\tilde{e}_i, v) = \tilde{r}_i(v), \quad v \in S_2(\Omega_i; \mathcal{T}_i^{(k)}), \tag{3.16}$$

$$\tilde{r}_i(v) := (f, v)_{0;\Omega_i} - a_i(u_m, v) + \int\limits_{\partial\Omega_i \setminus \partial\Omega} \lambda_m [v]_J \, d\sigma,$$

where v is extended to zero outside of Ω_i.

If we assume that the weak solution u is continuous on Ω, we can define Dirichlet boundary conditions of a discrete finite element solution pointwise on the nodal points on $\partial\Omega_i$. Let $u_{2,i} \in S_2(\Omega_i; \mathcal{T}_i^{(k)})$, $1 \le i \le N$, be the solution of the discrete Dirichlet boundary value problem on Ω_i

$$a_i(u_{2,i}, v) = (f, v)_{0;\Omega_i}, \quad v \in S_{2;0}(\Omega_i; \mathcal{T}_i^{(k)}), \tag{3.17}$$

where $S_{2;0}(\Omega_i; \mathcal{T}_i^{(k)}) := \{v \in S_2(\Omega_i; \mathcal{T}_i^{(k)}) \mid \ v|_{\partial\Omega_i} = 0\}$ and $u_{2,i}$ on the boundary $\partial\Omega_i$ is given by

$$u_{2,i}(x) := u(x),$$

where x is either a vertex or the midpoint of an edge on $\partial\Omega_i$. We impose a saturation assumption by requiring the existence of constants $0 \le \beta_i \le \beta$, $1 \le i \le N$, with β small enough and independent of the refinement level such that

$$|||\, u_{2,i} - u \,|||_{\Omega_i} \le \beta_i \,|||\, e_i \,|||_{\Omega_i}, \quad 1 \le i \le N, \tag{3.18}$$

where $|||\cdot|||_{\Omega_i} := a_i(\cdot,\cdot)^{1/2}$, $1 \le i \le N$. In the sequel, we will further refer to $|||\cdot|||_{\Omega} := (\sum_{i=1}^N |||\cdot|||_{\Omega_i}^2)^{1/2}$ as the broken energy norm associated with the bilinear form $a(\cdot,\cdot) = \sum_{i=1}^N a_i(\cdot,\cdot)$.

The solutions $\tilde{e}_i$ of (3.16) only provide a lower bound for the discretization error. In view of

$$|||\, e \,|||_{\Omega}^2 = \sum_{i=1}^N \tilde{r}_i(e_i) + \sum_{\ell=1}^L \int_{\Gamma_\ell} (\mathbf{n}\cdot a\nabla u - \lambda_m)[u_m]_J \, d\sigma, \tag{3.19}$$

we further have to take into account the jumps $[u_m]_J$ across the interfaces. It can be shown that

$$\left(\sum_{l=1}^L \sum_{E\subset\Gamma_l} h_E^{-1} \|[u_m]_J\|_{0;E}^2 \right)^{1/2}, \ h_E := |E|$$

is an appropriate tool for measuring the nonconformity of the mortar finite element solution.

To prove boths upper and lower bounds for the error in the broken energy norm we have to impose another saturation assumption concerning the approximation of the normal fluxes $\mathbf{n}\cdot a\nabla u$ on S by the multipliers from $M_1(S)$

$$\inf_{\mu\in M_1(S)} \|\mu - \mathbf{n}\cdot a\nabla u\|_{0;S} \le C \,|||\, u - u_m \,|||, \tag{3.20}$$

where $\|\cdot\|_{0;S}$ stands for the weighted L^2-norm

$$\|v\|_{0;S} := \left(\sum_{E\subset S} h_E \|v\|_{0;E}^2 \right)^{1/2}.$$

Remark 3.1. The saturation assumption (3.20) is motivated by a priori error estimates

$$|||\, u - u_m \,||| \le C \left(\sum_{i=1}^N h_i^2 \|u\|_{2;\Omega_i}^2 \right)^{1/2}$$

$$\inf_{\mu\in M_1(S)} \|\mu - \mathbf{n}\cdot a\nabla u\|_{0;S} \le C \left(\sum_{i=1}^N h_i^3 \|u\|_{2;\Omega_i}^2 \right)^{1/2}$$

which are due to Bernardi, Maday, and Patera [**8**], [**9**] and Ben Belgacem [**7**], respectively.

As a consequence of the saturation assumption (3.20) we have:

Lemma 3.1. *Suppose that* (3.20) *is satisfied. Then there holds*

$$\|\lambda_m - \mathbf{n}\cdot a\nabla u\|_{0;S} \le C \;|||\; e \;|||_\Omega \; . \tag{3.21}$$

For the proof of (3.21) *we refer to* [**31**].

Summarizing the preceding results, we obtain:

Theorem 3.1. *Under the saturation assumptions* (3.17) *and* (3.20)*, there holds*

$$c \;|||\; e \;|||_\Omega^2 \le \sum_{i=1}^{N} |||\; \tilde{e}_i \;|||_{\Omega_i}^2 + \sum_{l=1}^{L} \sum_{E\in\Gamma_l} h_E^{-1} \|[u_m]_J\|_{0;E}^2 \le C \;|||\; e \;|||_\Omega^2 \tag{3.22}$$

For a proof of Theorem 3.1 *we refer to* [**32**].

A localization of the Neumann problems (3.16) can be achieved by taking advantage of the hierarchical two-level splitting

$$S_2(\Omega_i;\mathcal{T}_i^{(k)}) = S_1(\Omega_i;\mathcal{T}_i^{(k)}) \oplus \tilde{S}_2(\Omega_i;\mathcal{T}_i^{(k)}), \tag{3.23}$$

where $\tilde{S}_2(\Omega_i;\mathcal{T}_i^{(k)})$ stands for the hierarchical surplus spanned by the quadratic nodal basis functions φ_E associated with $E\in\mathcal{E}_k^{\overline{\Omega}_i\setminus\Gamma}$.

Lemma 3.2. *Let* $\tilde{S}_2(\Omega_i;\mathcal{T}_i^{(k)}) = \operatorname{span}\{\varphi_E \mid E \in \mathcal{E}_k^{\overline{\Omega}_i\setminus\Gamma}\}$ *and* $\alpha_E := \tilde{r}_i(\varphi_E)/a_i(\varphi_E,\varphi_E)$, $1\le i\le N$, *with* $\tilde{r}_i(\cdot)$ *given by* (3.16)*. Then, for* $1\le i\le N$ *there holds*

$$c \sum_{E\in\mathcal{E}_k^{\overline{\Omega}_i\setminus\Gamma}} \alpha_E^2 \;|||\; \varphi_E \;|||_{\Omega_i}^2 \le ||| \;\tilde{e}_i\; |||_{\Omega_i}^2 \le C \sum_{E\in\mathcal{E}_k^{\overline{\Omega}_i\setminus\Gamma}} \alpha_E^2 \;|||\; \varphi_E \;|||_{\Omega_i}^2 \; . \tag{3.24}$$

Proof. The assertion follows from the strengthened Cauchy-Schwarz inequalities

$$a_i(v_i,w_i) \le q_1 \;|||\; v_i \;|||_{\Omega_i} |||\; w_i \;|||_{\Omega_i}, v_i\in S_1(\Omega_i;\mathcal{T}_i^{(k)}), \quad w_i \in \tilde{S}_2(\Omega_i;\mathcal{T}_i^{(k)}),$$

$$a_i(\varphi_E,\varphi_{E'}) \le q_2 \;|||\; \varphi_E \;|||_{\Omega_i} |||\; \varphi_{E'} \;|||_{\Omega_i}, \quad E,E'\in\mathcal{E}_k^{\overline{\Omega}_i\setminus\Gamma}, \quad E\neq E',$$

where $0\le q_\nu < 1$, $1\le \nu\le 2$, are independent of the refinement level (cf., e.g., [**16**]).

We are thus led to the following hierarchical type error estimator

$$\begin{aligned} \eta_H &:= \left(\sum_{T\in\mathcal{T}_k} \eta_{H;T}^2\right)^{1/2}, \\ \eta_{H;T}^2 &:= \sum_{E\in\mathcal{E}_k(T)} \alpha_E^2 \;|||\; \varphi_E \;|||^2 + \sum_{l=1}^{L} \sum_{E\in\mathcal{E}_k(T)\cap\Gamma_l} h_E^{-1}\|[u_m]_J\|_{0;E}^2, \; T\in\mathcal{T}_k. \end{aligned} \tag{3.25}$$

The preceding results imply that η_H delivers a lower and an upper bound for the broken energy norm of the discretization error.

Theorem 3.2. *Let η_H be the hierarchical error estimator as given by* (3.25). *Then, under the saturation assumptions* (3.17) *and* (3.20) *there exist constants* $0 < \gamma_H \leq \Gamma_H$ *depending only on the shape regularity of* $\mathcal{T}_0$ *and on* $\underline{\alpha}, \overline{\alpha}, \underline{\beta}, \overline{\beta}$ *in* (1.3), (1.4) *such that*

$$\gamma_H \eta_H \leq ||| \, e \, ||| \leq \Gamma_H \eta_H . \tag{3.25}$$

Proof. The assertion follows readily from Theorem 3.1 and Lemma 3.3. □

Remark 3.2. In practice, we only have iterative approximations $(\tilde{u}_m, \tilde{\lambda}_m)$ for the exact solution (u_m, λ_m) of (3.8), (3.9) at hand. Then, the iteration errors $||| \, u_m - \tilde{u}_m \, |||$ and $\|\lambda_m - \tilde{\lambda}_m\|_{0;S}$ also enter the bounds in (3.26). We remark that, due to the optimality of the iterative solvers described in subsection 3.2, the iteration errors can be controlled during the iterative solution process by monitoring the residuals with respect to the computed iterates.

Remark 3.3.. We note that residual based a posteriori error estimators for mortar finite element discretizations have been developed in [**17**], [**31**]. The hierarchical basis error estimator and a fully hierarchical basis error estimator that includes the error $(\mathbf{n} \cdot a\nabla u)$ have been analyzed in [**32**].

4. Numerical Results

In this section, we present some numerical results illustrating the benefits of the adaptive mixed and the adaptive macro-hybrid finite element methods.

As an example for the mixed hybrid approach, we consider (1.1) with $a = 1.0$ and $b = 0.25$ and homogeneous Dirichlet boundary on the three dimensional unit cube $\Omega = (0,1)^3$ where the right-hand side f has been chosen such that $u(\mathbf{x}) = 1000 \cdot \exp(-100((x-0.4)^2 + (y-0.2)^2 + (z-0.3)^2)) \cdot x(x-1)y(y-1)z(z-1)$ is the solution of the problem. Note that u exhibits an exponential peak at the interior point $\mathbf{x} = (0.4, 0.2, 0.3)^T$. We solve the problem by mixed hybridization with respect to a hierarchy of adaptively generated hexalateral triangulations using the multilevel preconditioned cg-iteration as described in subsection 2.2 and local adaptive grid refinement based on the a posteriori error estimator of subsection 2.3. Nonconforming nodal points arising from the adaptive refinement process have been treated in the usual way as hanging nodes.

Figure 4.1 shows the adaptively generated final triangulation at different clipping planes whereas Table 4.1 contains the history of the refinement process by displaying the number of unknowns, the estimated and true errors as well as the effectivity index for each refinement level. Note that the effectivity index is the ratio of the estimated and the true error. We can see that there is a pronounced refinement in the vicinity of the exponential peak and we also observe that the effectivity index rapidly approaches its optimal value 1.

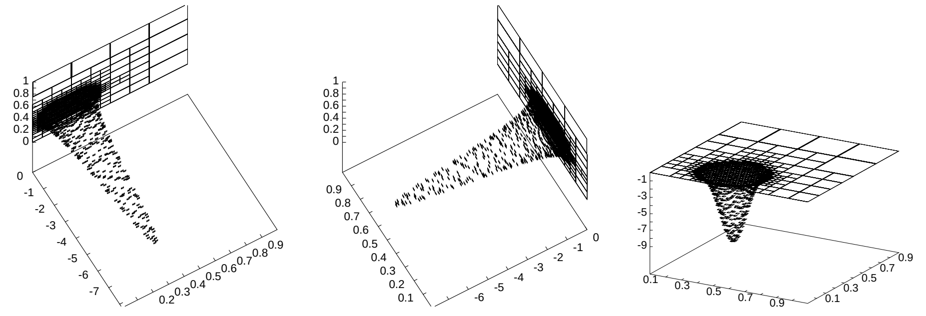

$x = 0.4\,\text{cm}$ $y = 0.2\,\text{cm}$ $z = 0.3\,\text{cm}$

Figure 4.1. Final triangulation.

Level	# Nodes	Error	Est. Error	Eff. Index
0	20	0.328555	0.0328704	0.118
1	208	0.322324	0.1057	0.328
2	886	0.195379	0.133779	0.685
3	2186	0.113028	0.0963011	0.852
4	9874	0.0573235	0.0548544	0.957
5	59267	0.0287311	0.0283626	0.987

Table 4.1. Effectivity index.

A real-life application of the algorithm, namely the simulation of the neutron kinetics of a nuclear power plant, can be found in [**10**].

The second example concerns the performance of the hierarchical type error estimator for adaptive mortar finite element methods. We consider a problem on a domain with a reentrant corner (cf. Figure 4.2a) where $a = 1$, $b = 100$ and f is chosen such that $u = r^{\frac{2}{3}} \sin(\frac{2}{3}\phi)$ is the solution of the problem. We have further investigated a diffusion equation in $\Omega = (0,1)^2$ with a discontinuous coefficient ($a = 1$ in $\Omega_1 := \{(x,y) \subset \Omega \mid x < 1/2,\ x < y < 1 - x$ or $x > 1/2,\ x > y > 1 - x\}$ and $a = 100$ elsewhere) with the solution $u(x,y) = (x-y)(1-x-y)$. We have solved both problems with respect to an adaptively generated simplicial triangulation using a preconditioned Lanczos iteration with substructuring multilevel preconditioners of BPX-type (cf. subsection 3.2) and we have used the hierarchical error estimator described in subsection 3.3.

The history of the refinement process is given by Tables 4.2a and 4.2b. We again observe that the effectivity index quickly approaches 1. Figures 4.2a and 4.2b show the adaptively generated final triangulation in the two cases.

Level	# Nodes	Est. Error	Error	Eff. Index
0	24	0.265	0.313	0.847
1	50	0.137	0.142	0.965
2	100	$0.891{\cdot}10^{-1}$	$0.939{\cdot}10^{-1}$	0.952
3	154	$0.651{\cdot}10^{-1}$	$0.676{\cdot}10^{-1}$	0.963
4	277	$0.455{\cdot}10^{-1}$	$0.470{\cdot}10^{-1}$	0.969
5	599	$0.314{\cdot}10^{-1}$	$0.321{\cdot}10^{-1}$	0.976
6	1069	$0.217{\cdot}10^{-1}$	$0.221{\cdot}10^{-1}$	0.981
7	2342	$0.143{\cdot}10^{-1}$	$0.145{\cdot}10^{-1}$	0.981
8	5190	$0.957{\cdot}10^{-2}$	$0.975{\cdot}10^{-2}$	0.981
9	11510	$0.631{\cdot}10^{-2}$	$0.641{\cdot}10^{-2}$	0.984

Table 4.2a. Reentrant corner.

Level	# Nodes	Est. Error	Error	Eff. Index
0	24	0.241	0.408	0.592
1	60	0.150	0.147	1.02
2	116	$0.764{\cdot}10^{-1}$	$0.759{\cdot}10^{-1}$	1.01
3	320	$0.392{\cdot}10^{-1}$	$0.393{\cdot}10^{-1}$	0.997
4	1150	$0.196{\cdot}10^{-1}$	$0.197{\cdot}10^{-1}$	0.998
5	4372	$0.100{\cdot}10^{-1}$	$0.991{\cdot}10^{-2}$	1.01
6	17044	$0.497{\cdot}10^{-2}$	$0.495{\cdot}10^{-2}$	1.00

Table 4.2b. Discontinuous coefficient.

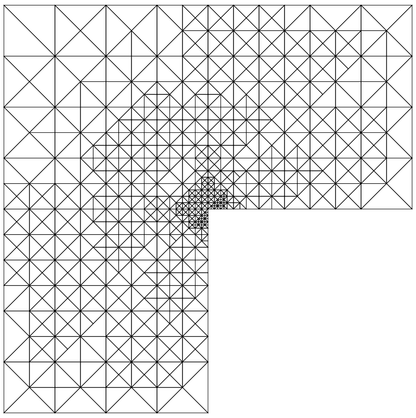

Figure 4.2a. Reentrant corner.

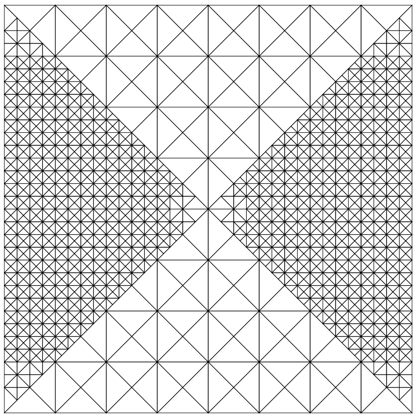

Figure 4.2b. Discontinuous coefficient.

For further numerical results, including fully potential flows around airfoils we refer to [**17**], [**31**], [**32**].

References

1. Achdou Y. and Kuznetsov Yu. A., *Substructuring preconditioners for finite element methods on nonmatching grids*, East-West J. Numer. Math. **3** (1995), 1–28.
2. Achdou Y., Maday Y. and Widlund O., *Méthode iterative de sous-structuration pour les éléments avec joints*, C. R. Acad. Sci., Paris, Sér. I **322** (1996), 185–190.
3. ______, *Iterative Substructuring Preconditioners for Mortar Element Methods in Two Dimensions*, Tech. Report 735, Courant Institute of Math. Sciences, New York.
4. Arbogast T., Cowsar L. C, Wheeler M. F. and Yotov I., *Mixed finite element methods on non-matching multiblock grids*, submitted to SIAM J. Num. Anal..
5. Arnold D. N. and Brezzi F., *Mixed and nonconforming finite element methods: implementation, post-processing, and error estimates*, M^2AN Math. Modelling Numer. Anal. **19** (1985), 7–35.
6. Bank R. E. and Weiser A., *Some a posteriori error estimators for elliptic partial differential equations*, Math. Comput. **44** (1985), 283–301.
7. Ben Belgacem F., *The mortar finite element method with Lagrange multipliers*, submitted to Numer. Math..
8. Bernardi C., Maday Y. and Patera A., *A new nonconforming approach to domain decomposition: the mortar element method*, Nonlinear Partial Differential Equations and Their Applications (J. L. Lions and H. Brézis, eds.), Pitman, Boston, 1994, pp. 13–51.
9. ______, *Domain decomposition by the mortar element method*, Asymptotic and Numerical Methods for Partial Differential Equations with Critical Parameters (H.Kaper et al., eds.), Reidel, Dordrecht, 1993, pp. 269–286.
10. Boer R. and Finnemann H., *Fast analytical flux reconstruction method for nodal space-time nuclear reactor analysis*, Ann. Nucl. Energy **19** (1992), 617–628.
11. Bramble J., Pasciak J. and Xu J., *Parallel multilevel preconditioners*, Math. Comput. **55** (1990), 1–22.
12. Brandts J., *Superconvergence and a posteriori error estimation for triangular mixed finite elements.*
13. Brenner S., *A multigrid algorithm for the lowest-order Raviart-Thomas mixed triangular finite element method.*, SIAM J. Numer. Anal. **29** (1992), 647–678.
14. Brezzi F. and Fortin M., *Mixed and Hybrid Finite Element Methods*, Springer, Berlin – Heidelberg – New York, 1991.
15. Brezzi F. and Marini L., *A three-field domain decomposition method*, Proc. 6th Int. Symp. on Domain Decomposition Methods for PDEs (Yu. A. Kuznetsov, J. Périaux, A. Quarteroni and O. Widlund, eds.), Amer. Math. Soc., Providence, 1994, pp. 27–34.
16. Deuflhard P., Leinen P. and Yserentant H., *Concepts of an adaptive hierarchical finite element code*, IMPACT Comput. Sci. Engrg. **1** (1989), 3–35.
17. Engelmann B., Hoppe R. H. W., Iliash Yu., Kuznetsov Yu. A., Vassi-Levski Y. and B. Wohlmuth, *Efficient parallel solvers for potential flow and convection-diffusion problems on nonmatching grids*, Techn. Report, Inst. of Math., Univ. of Augsburg, 1997.
18. Fraeijs De Veubeke B., *Displacement and equilibrium models in the finite element method*, Stress Analysis (C. Zienkiewicz and G. Holister, eds.), Wiley, Chichester, 1965.
19. Hennart J. P., *A general family of nodal schemes*, SIAM J. Sci. Stat. Comput. **7** (1986), 264–287.
20. Hoppe R. H. W. and Wohlmuth B., *Adaptive multilevel iterative techniques for nonconforming finite element discretizations*, East-West J. Numer. Math. **3** (1995), 179–197.
21. ______, *Element-oriented and edge-oriented local error estimators for nonconforming finite element methods*, M^2AN Math. Modeling and Numer. Anal. **30** (1996), 237–263.
22. ______, *Multilevel iterative solution and adaptive mesh refinement for mixed finite element discretizations*, Appl. Numer. Math. **23** (1997), 97–117.
23. Kuznetsov Yu. A., *Efficient iterative solvers for elliptic finite element problems on nonmatching grids*, Russ. J. Numer. Anal. Math. Modelling **10** (1995), 187–211.

24. Le Tallec P., *Neumann-Neumann domain decomposition algorithms for solving 2D elliptic problems with nonmatching grids*, East-West J. Numer. Math. **1** (1993), 129–146.

25. Nepomnyaschikh S. V., *Fictitious components and subdomain alternating methods*, Sov. J. Numer. Anal. Math. Modelling **5** (1990), 53–68.

26. Oswald P., *On a BPX-preconditioner for P1 elements*, Computing **51** (1993), 125–133.

27. Rannacher R. and Turek S., *A simple nonconforming quadrilateral Stokes element*, Numer. Meth. Part. Diff. Equ. **8** (1992), 97–11.

28. Sarkis M., *Multilevel methods for P1 nonconforming finite elements and discontinuous coefficients in three dimensions*, Proc. 7th Int. Symp. on Domain Decomposition Methods for PDEs (D. E. Keyes et al., eds.), Amer. Math. Soc., Providence, 1994, pp. 119–124.

29. Verfürth R., *A posteriori error estimation and adaptive mesh-refinement techniques*, J. Comp. Appl. Math. **50** (1994), 67–83.

30. ______, *A Review of A Posteriori Error Estimation and Adaptive Mesh-Refinement Techniques*, Wiley-Teubner, Chichester-Stuttgart, 1996.

31. Wohlmuth B., *A residual based error estimator for mortar finite element discretizations*, Techn. Report 370, Inst. of Math., Univ. of Augsburg, 1997.

32. ______, *Hierarchical a posteriori error estimators for mortar finite element methods with Lagrange multipliers*, Tech. Report 749, Courant Institute of Math. Sciences, New York University, 1997.

33. Xu J., *Iterative methods by space decomposition and subspace correction*, SIAM Rev. **34** (1992), 581–613.

R. H. W. Hoppe, Institute of Mathematics, University of Augsburg, Universitätsstrasse 14, D-86159 Augsburg, Germany; *e-mail:* hoppe@math.uni-augsburg.de

B. I. Wohlmuth, Courant Institute of Mathematical Sciences, 251 Mercer Street, New York, N.Y. 10012, USA and Institute of Mathematics, University of Augsburg, D-86135 Augsburg, Germany; *e-mail* wohlmuth@cs.nyu.edu, wohlmuth@math.uni-augsburg.de